Supplementary Information

Facile and rapid fabrication of porous CuBr films by a solution oxidation and their application for the exclusive detection of NH_3 at room temperature

Sang-Kwon Kim,[a] Byeong-Hun Yu,[a] Chan Woong Na,[b] Jong-Heun Lee,[c] and Ji-Wook Yoon[a,*]

[a]*Department of Information Materials Engineering, Division of Advanced Materials Engineering, Jeonbuk National University, Jeonju 54896, Republic of Korea.*

[b]*Dongnam Division, Korea Institute of Industrial Technology, Busan 46938, Republic of Korea*

[c]*Department of Materials Science and Engineering, Korea University, Seoul 02841, Republic of Korea.*

E-mail: jwyoon@jbnu.ac.kr (Ji-Wook Yoon)

SUPPLEMENTARY FIGURES

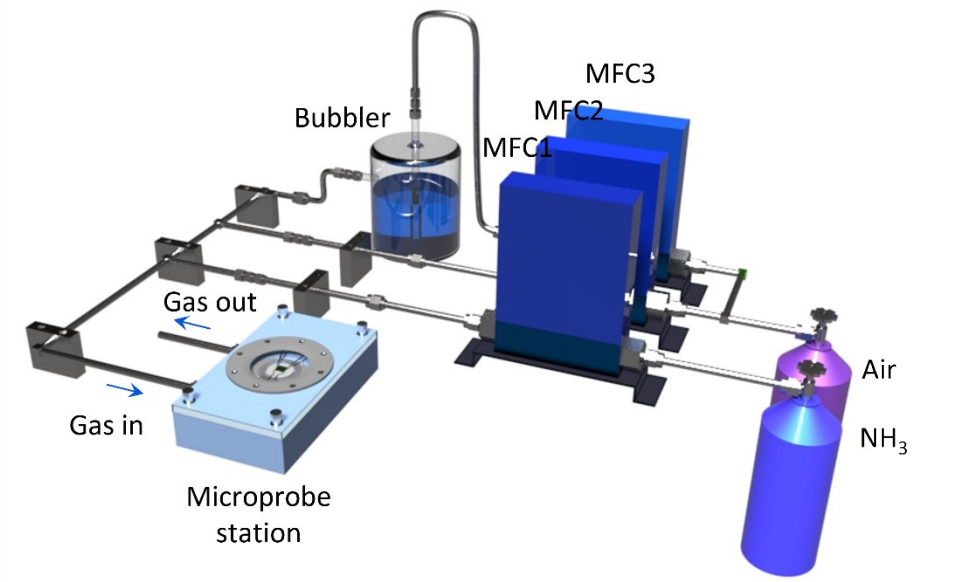

MFC	MFC1 (mL min^{-1})	MFC2 (mL min^{-1})	MFC3 (mL min^{-1})
Gas	**5 ppm NH_3**	**Dry air**	**Dry air + Bubbler**
5 ppm NH_3	500	0	0
0.5 ppm NH_3	50	450	0
0.5 ppm NH_3 in r.h.20%	50	350	100
0.5 ppm NH_3 in r.h.50%	50	200	250
0.5 ppm NH_3 in r.h.80%	50	50	400

Fig. S1 Setup and flow configuration for gas sensing test.

SUPPLEMENTARY FIGURES

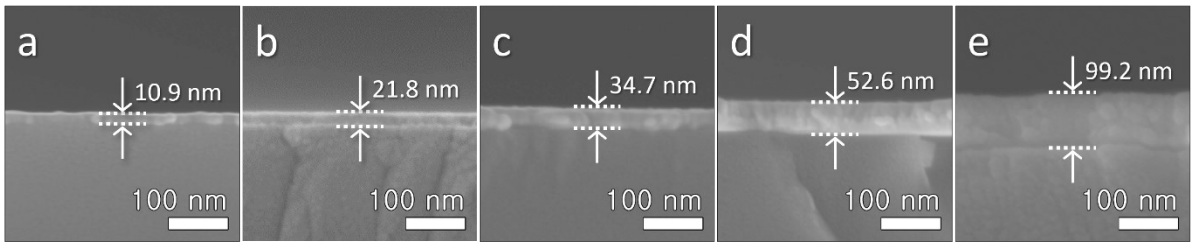

Fig. S2 SEM images of cross-sectional views of the Cu films prepared by sputtering.

SUPPLEMENTARY FIGURES

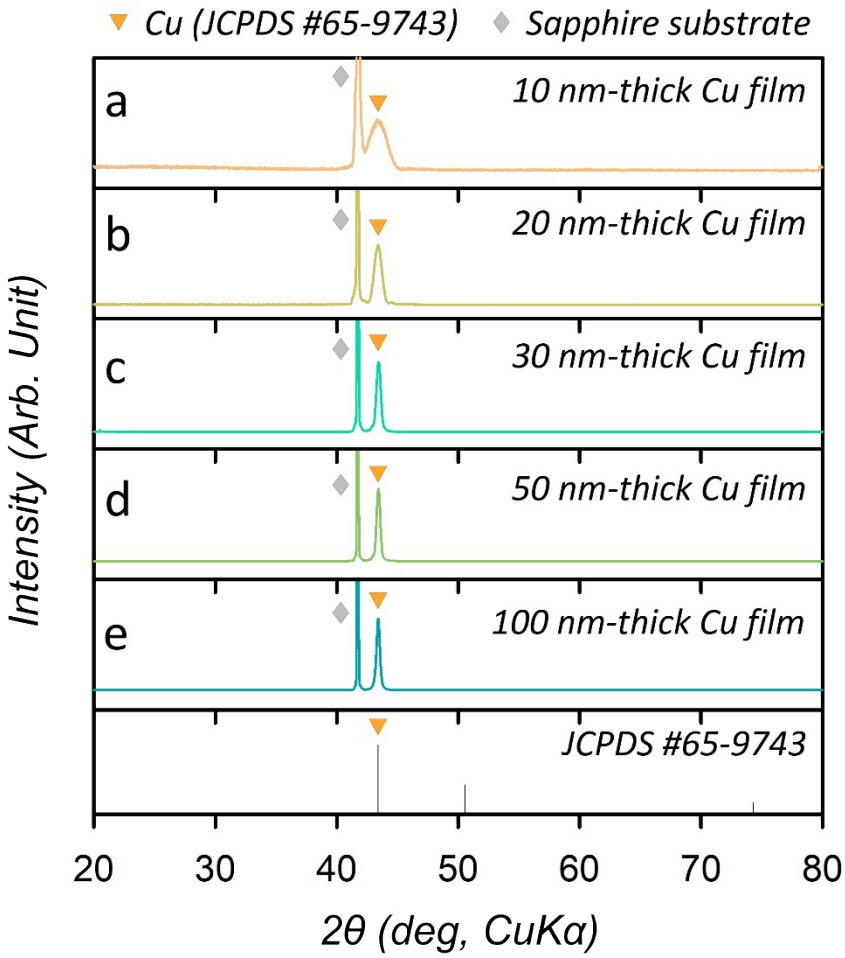

Fig. S3 XRD patterns of the Cu films prepared by sputtering.

SUPPLEMENTARY FIGURES

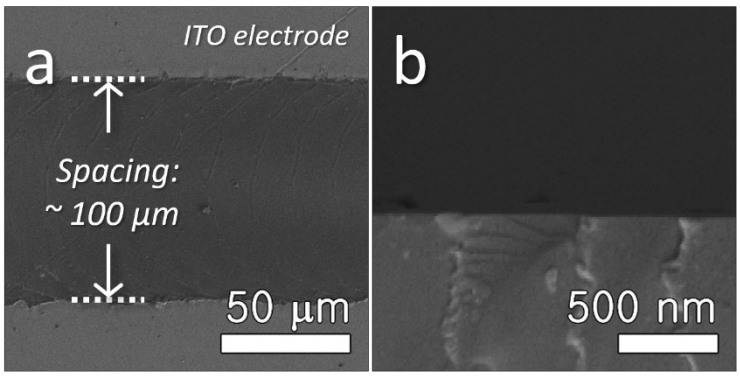

Fig. S4 SEM images of top (a) and cross-sectional (b) views of the 10n-120s sensor. CuBr particles were rarely observed on the sensor substrate after oxidation in solution.

SUPPLEMENTARY FIGURES

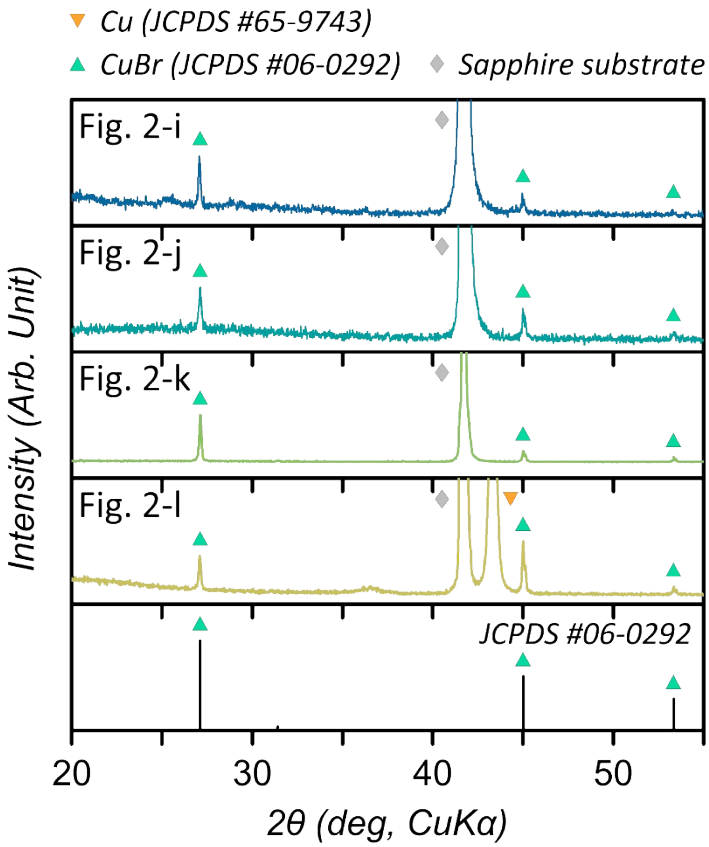

Fig. S5 XRD pattern of the CuBr films prepared by immersing 20 – 100 nm-thick Cu films in the $CuBr_2$ solutions for 120 s.

SUPPLEMENTARY FIGURES

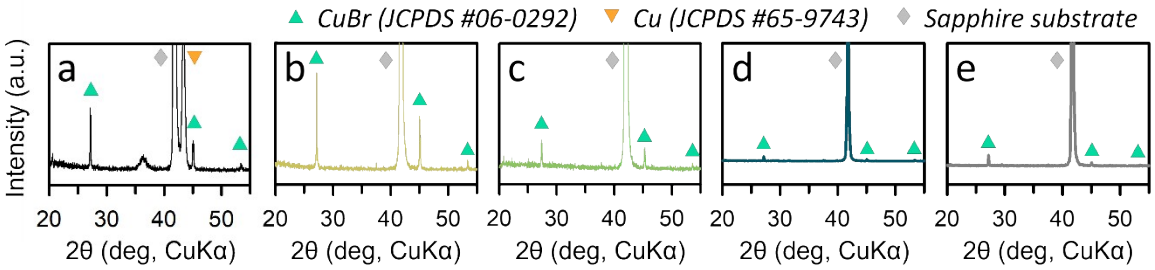

Fig. S6 XRD pattern of the CuBr film prepared by immersing 30 nm-thick Cu films in the $CuBr_2$ solutions for 10 – 300 s: (a) 30n-10s, (b) 30n-30s, (c) 30n-60s, (d) 30n-180s, and (e) 30n-300s. All the specimens consisted of CuBr, whereas the 30n-10s specimen additionally contained Cu.

SUPPLEMENTARY FIGURES

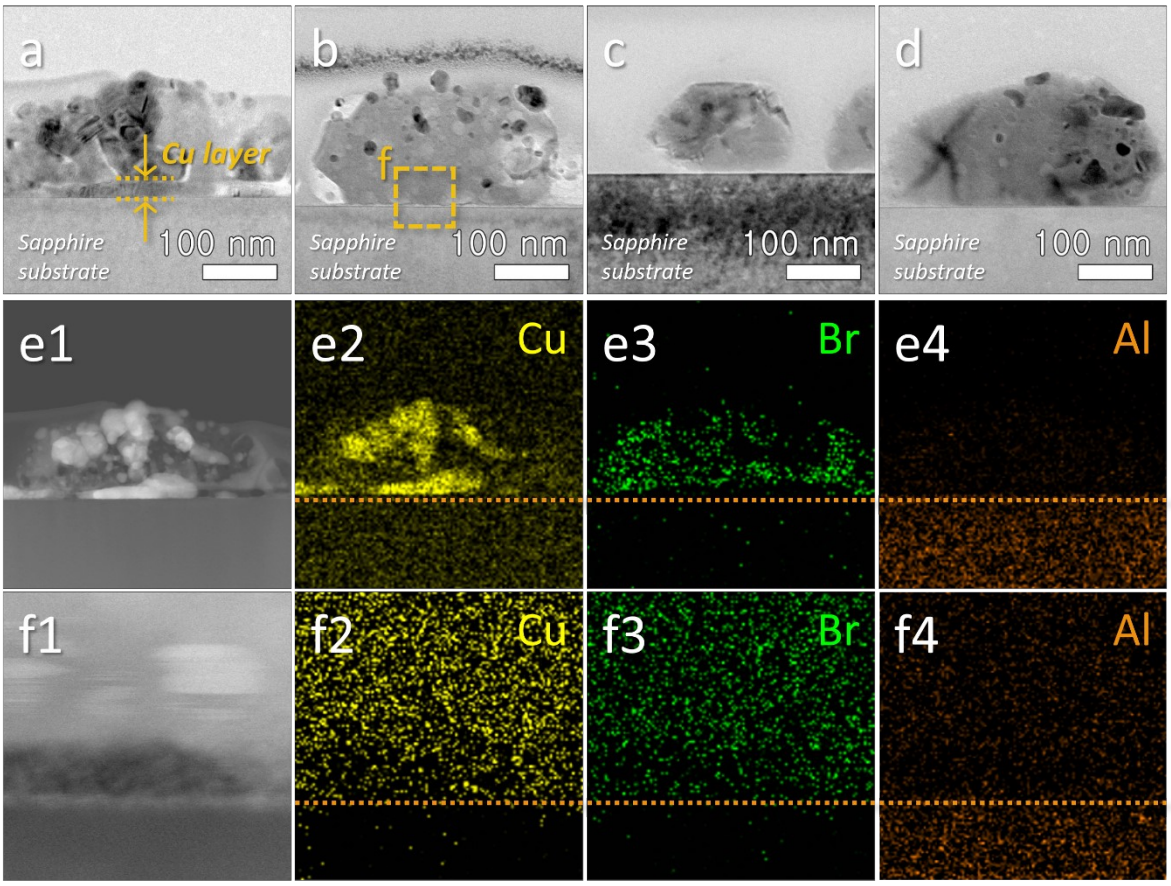

Fig. S7 TEM images of the FIB-treated CuBr film prepared by immersing 30 nm-thick Cu films in the $CuBr_2$ solutions for (a) 10, (b) 30, (c) 60, and (d) 120 s. Elemental mapping images for the FIB-treated 30n-10s (e) and 30n-30s (f). This clearly shows that the oxidation of Cu to Cu^+ in CuBr was complete within 30 s.

SUPPLEMENTARY FIGURES

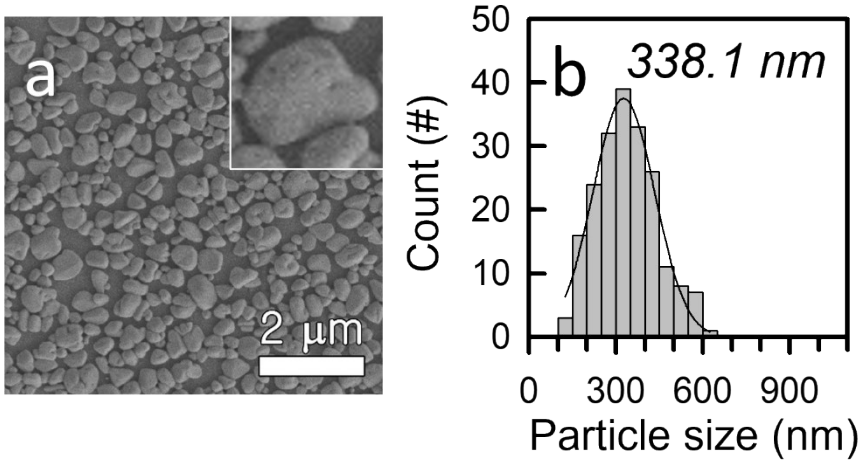

Fig. S8 (a) SEM image and (b) particle size distribution of the 30n-10s film.

SUPPLEMENTARY FIGURES

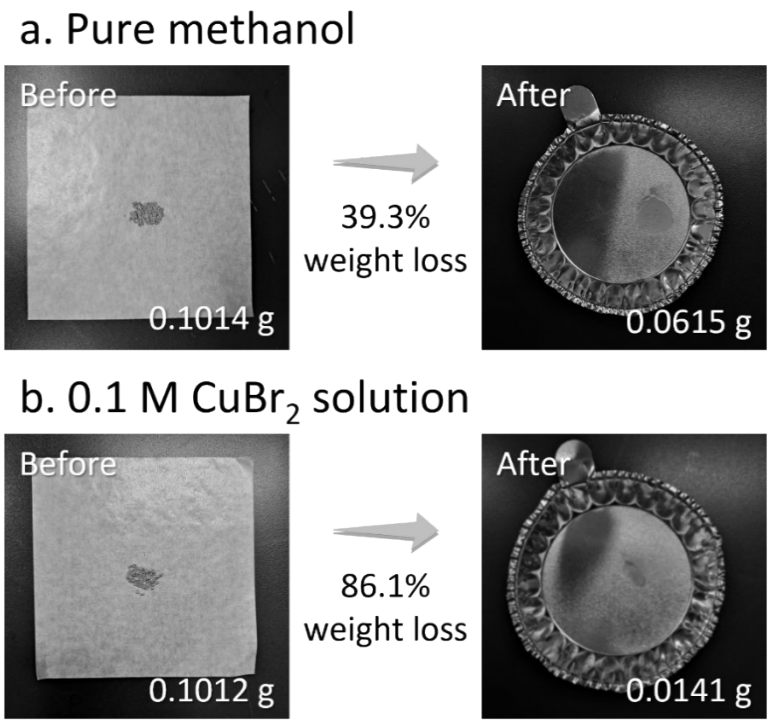

Fig. S9 Weight loss of commercial CuBr powders measured after dissolving in (a) pure methanol and (b) 0.1 M $CuBr_2$ solution for 3 h. The weight loss of CuBr powders in 0.1 M $CuBr_2$ solution (86.1%) was significantly higher than that in pure methanol (39.3%).

SUPPLEMENTARY FIGURES

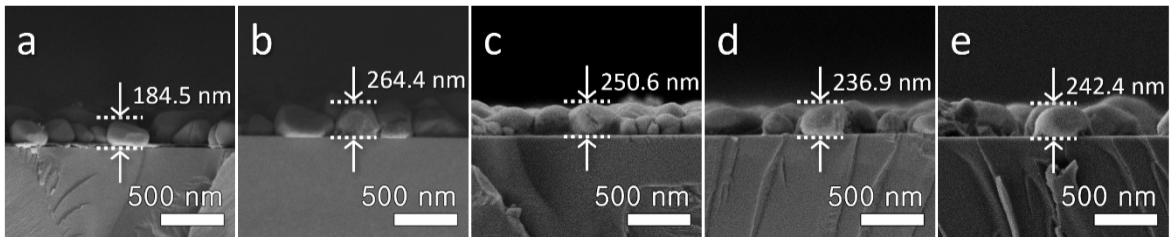

Fig. S10 Cross-sectional SEM images of the 30n-10s (a), 30n-30s (b), 30n-60s (c), 30n-180s (d), and 30n-300s (e) specimens.

SUPPLEMENTARY FIGURES

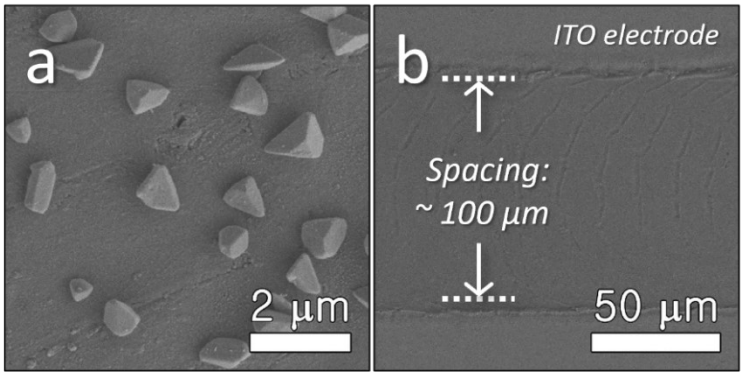

Fig. S11 SEM images of the CuBr films prepared by immersing 30 nm-thick Cu films in (a) 0.001 M and (b) 0.1 M for 120 s.

SUPPLEMENTARY FIGURES

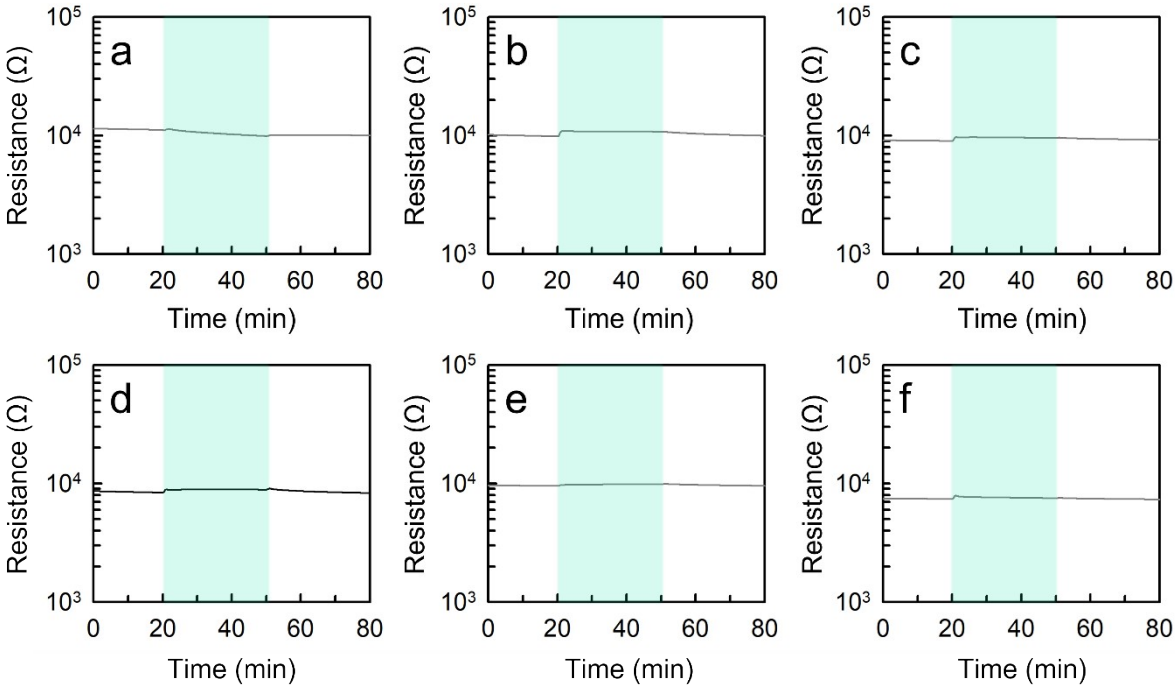

Fig. S12 Resistance changes of the 30n-120s sensor upon exposure to 5 ppm (a) NO_2, (b) acetone, (c) CO, (d) ethanol, (e) acetaldehyde, and (f) formaldehyde.

SUPPLEMENTARY FIGURES

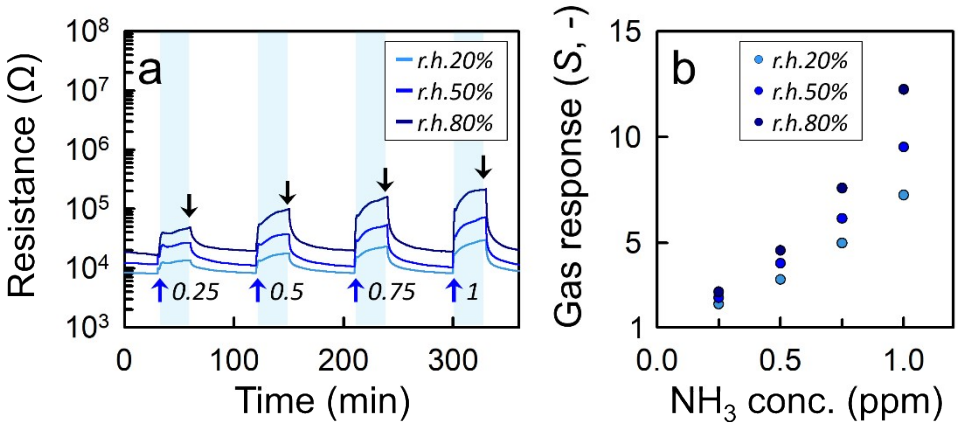

Fig. S13 (a) Resistance changes and (b) gas response of the 30n-120s sensor to 0.25 – 1 ppm NH_3 at various humidity levels.

SUPPLEMENTARY FIGURES

Table S1 Comparison of our CuBr sensor with those reported in the literature.

Structure	Synthesis method	Synthesis temperature (℃)	Response (-)	Conc. (ppm)	Humidity condition	Ref.
Particles	Powder mixing	RT	12.7	5	Dry	27
Dense film	Solution oxidation	RT	5.5	1	-	43
	RF sputtering	RT	20	5	dry	44
	RF sputtering	RT	8	10	dry	45
	RF sputtering	RT	12	10	dry	46
Porous film	Flame pyrolysis and dry bromination	1500-2000	276	5	dry	26
			20	1	r.h. 90%	
	Thermal evaporation	500	220	5	dry	30
			12	1	r.h. 80%	
	Solution oxidation	RT	12	10	dry	35
	Solution oxidation	RT	211	5	dry	This work
			12.2	1	r.h. 80%	This work